

Peierls-phase-induced topological semimetals in an optical lattice: Moving of Dirac points, anisotropy of Dirac cones, and hidden symmetry protection
Jing-Min Hou(侯净敏)
Citation: Chin. Phys. B, 2020, 29 (**12**): 120305. DOI: 10.1088/1674-1056/abc0de
Journal homepage: http://cpb.iphy.ac.cn; http://iopscience.iop.org/cpb

What follows is a list of articles you may be interested in

Zitterbewegung of Dirac quasiparticles emerged in a Su-Schrieffer-Heeger lattice
Yue Hu(胡玥), Zheng-Xin Guo(郭政鑫), Ze-Ming Zhong(钟泽明), and Zhi Li(李志)
Chin. Phys. B, 2020, 29 (**11**): 110302. DOI: 10.1088/1674-1056/abb45b

Cyclotron dynamics of neutral atoms in optical lattices with additional magnetic field and harmonic trap potential
Ai-Xia Zhang(张爱霞), Ying Zhang(张莹), Yan-Fang Jiang(姜艳芳), Zi-Fa Yu(鱼自发), Li-Xia Cai(蔡丽霞), Ju-Kui Xue(薛具奎)
Chin. Phys. B, 2020, 29 (**1**): 010307. DOI: 10.1088/1674-1056/ab5efc

Periodically modulated interaction effect on transport of Bose-Einstein condensates in lattice with local defects
Kun-Qiang Zhu(朱坤强), Zi-Fa Yu(鱼自发), Ji-Ming Gao(高吉明), Ai-Xia Zhang(张爱霞), Hong-Ping Xu(徐红萍), Ju-Kui Xue(薛具奎)
Chin. Phys. B, 2019, 28 (**1**): 010307. DOI: 10.1088/1674-1056/28/1/010307

Tunable ground-state solitons in spin-orbit coupling Bose-Einstein condensates in the presence of optical lattices
Huafeng Zhang(张华峰), Fang Chen(陈方), Chunchao Yu(郁春潮), Lihui Sun(孙利辉), Dahai Xu(徐大海)
Chin. Phys. B, 2017, 26 (**8**): 080304. DOI: 10.1088/1674-1056/26/8/080304

Evolution of the vortex state in the BCS-BEC crossover of a quasi two-dimensional superfluid Fermi gas
Xuebing Luo(罗学兵), Kezhao Zhou(周可召), Zhidong Zhang(张志东)
Chin. Phys. B, 2016, 25 (**11**): 110306. DOI: 10.1088/1674-1056/25/11/110306

RAPID COMMUNICATION

Peierls-phase-induced topological semimetals in an optical lattice: Moving of Dirac points, anisotropy of Dirac cones, and hidden symmetry protection

Jing-Min Hou(侯净敏)†

School of Physics, Southeast University, Nanjing 211189, *China*

(Received 14 July 2020; accepted manuscript online 14 October 2020)

We propose a square optical lattice in which some of neighbor hoppings have a Peierls phase. The Peierls phase makes the lattice have a special band structure and induces the existence of Dirac points in the Brillouin zone, which means that topological semimetals exist in the system. The Dirac points move with the change of the Peierls phase and the Dirac cones are anisotropic for some vales of the Peierls phase. The lattice has a novel hidden symmetry, which is a composite antiunitary symmetry composed of a translation operation, a sublattice exchange, a complex conjugation, and a local $U(1)$ gauge transformation. We prove that the Dirac points are protected by the hidden symmetry and perfectly explain the moving of Dirac points with the change of the Peierls phase based on the hidden symmetry protection.

Keywords: topological semimetal, optical lattice, hidden symmetry

PACS: 03.75.Ss, 02.20.−a, 03.65.Vf, 05.30.Fk **DOI:** 10.1088/1674-1056/abc0de

1. Introduction

Presently, topological matters are important themes in condensed matters.[1,2] Among them, topological semimetals as gapless topological matters attract much attention of physicists.[3–8] Topological semimetals have band-touching points in Brillouin zone. Near the band-touching points, the dispersion relations are linear, which leads to the cone-like energy bands. the quasiparticles satisfy the Dirac (Weyl) equation and the quasiparticles are considered as Dirac (Weyl) fermions, so the band-touching points and the cone-like energy bands are called as Dirac (Weyl) points and Dirac (Weyl) cones, respectively.

In the last two decades, ultracold atom techniques have been tremendously developed and the high controllablity and high accuracy make them become a platform to study many interesting physics in condensed matters.[9–12] Concretely, ultracold atoms in optical lattices have been used to explore strongly correlated many-body systems of bosonic or fermionic particles, such as the superfluid–Mott phase transition of the Bose–Hubbard model.[13–15] The experimental realizations of artificial gauge potentials experienced by neutral atoms allow the investigation of new physical regimes,[16–19] such as quantum Hall effect. Quantum magnetism has been simulated with ultracold atoms in optical lattices.[20–24] The development of ultracold atom techniques also provides new opportunities to study topological semimetals in optical lattices,[25–32] especially, some of which are hardly realized in solid real materials.

In this paper, we consider a square optical lattice where some of neighbor hoppings have a hopping-accompanying phase, i.e., a Peierls phase.[19] When the value of the Peierls phase is in the range $(0, 2\pi)$, the energy bands have two Dirac points at some positions of the Brillouin zone. The two Dirac points have opposite topological charges. The positions of the Dirac points are dependent on the value of the Peierls phase, that is to say, the Dirac points move in the Brillouin zone when the Peierls phase changes. When the Peierls phase is π, the Dirac cones are isotropic, and when the Peierls phase has other values, the Dirac cones are anisotropic. We define an anisotropy factor for the Dirac cones and find that the anisotropy factor is dependent on the Peierls phase. It is intriguing that the lattice has a special hidden symmetry, which is a composite antiunitary symmetry composed of a translation operation, a sublattice exchange, a complex conjugation, and a local $U(1)$ gauge transformation. It is shown that the Dirac points are protected by the hidden symmetry and the moving of the Dirac points in the Brillouin zone with the Peierls phase varying can be perfectly explained by the hidden symmetry protection.

2. Model and hidden symmetry

Here, we consider ultracold atoms in a square optical lattice as shown schematically in Fig. 1(a). In this lattice, some of neighbor hoppings are accompanied by a Peierls phase with the value $0 < \gamma < 2\pi$, so that the translation symmetry is broken and the lattice is divided into two sublattices denoted as

†Corresponding author. E-mail: jmhou@seu.edu.cn

© 2020 Chinese Physical Society and IOP Publishing Ltd

A and B. The corresponding tight-binding Hamiltonian can be written as

$$H = -t\sum_{i\in A}[a_i^\dagger b_{i+\hat{x}} + a_i^\dagger b_{i-\hat{x}} + a_i^\dagger b_{i+\hat{y}} + \mathrm{e}^{\mathrm{i}\gamma} a_i^\dagger b_{i-\hat{y}}] + \mathrm{H.c.}, \quad (1)$$

where a_i destructs a particle at the site i in sublattice A and b_j destructs a particle at site j in sublattice B; $\hat{x} \equiv (1,0)$ and $\hat{y} \equiv (0,1)$ represent the unit vectors in the x and y directions, respectively; and t is the hopping amplitude along the x and y directions.

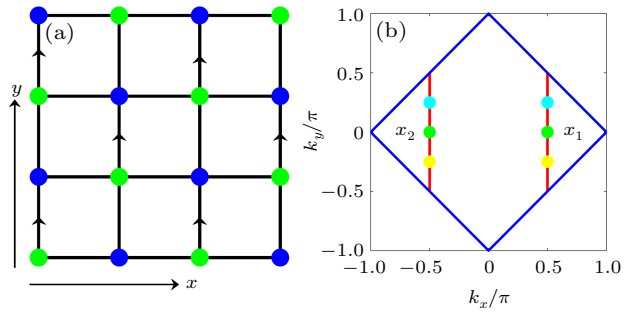


Fig. 1. (a) Schematic of the optical lattice. The arrows represent the Peierls phase γ; the blue and green filled circles represent the lattice sites of sublattices A and B, respectively. (b) The first Brillouin zone, which is surrounded by blue lines. Here, the red lines indicate the moving path of Dirac points $X_{1,2}$ when the Peierls phase varies in the range $(0, 2\pi)$; the yellow, green, and cyan filled circles indicate the locations of Dirac points $X_{1,2}$ for the cases $\gamma = \pi/2, \pi$, and $3\pi/2$, respectively.

For the translation-symmetry-breaking lattice, the Bravais lattice vector can be expressed as $\boldsymbol{R}_n = n_1\boldsymbol{a}_1 + n_2\boldsymbol{a}_2$, where $\boldsymbol{a}_1 = \hat{x} - \hat{y}$ and $\boldsymbol{a}_2 = \hat{x} + \hat{y}$ are the basis vectors of the Bravais lattice and n_1 and n_2 are integers. We chose a lattice site in sublattice A as the origin, then the lattice sites in sublattice A and sublattice B can be written as $\boldsymbol{R}_n^A = \boldsymbol{R}_n$ and $\boldsymbol{R}_n^B = \boldsymbol{R}_n + \hat{x}$. In the reciprocal lattice, the reciprocal lattice vector is defined as $\boldsymbol{K}_m = m_1\boldsymbol{b}_1 + m_2\boldsymbol{b}_2$, where m_1 and m_2 are integers, and $\boldsymbol{b}_1 = (\pi, -\pi)$ and $\boldsymbol{b}_2 = (\pi, \pi)$ are the corresponding primitive reciprocal lattice vectors. Due to the Peierls-phase-induced breaking of the translation symmetry, the unit cell of the square lattice is enlarged by two times and the corresponding Brillouin zone shrinks to one half as shown in Fig. 1(b).

Although the Peierls phase breaks the translation symmetry, the model still preserves a novel hidden symmetry. The hidden symmetry is a discrete symmetry with an antiunitary compositor operator as

$$\Upsilon = (\mathrm{e}^{\mathrm{i}\gamma})^{i_y}\sigma_x K T_{\hat{x}}, \quad (2)$$

where $T_{\hat{x}}$ is a translation operator which moves the lattice by $\hat{x}$ along the x direction; K is the complex conjugation operator, which can also be regarded as a time-reversal operator for spinless particles; σ_x is the Pauli matrix representing the sublattice exchange; and $(\mathrm{e}^{\mathrm{i}\gamma})^{i_y}$ is a $U(1)$ local gauge transformation. As shown in Fig. 2, the lattice keeps invariant after it is sequentially operated by the translation operation $T_{\hat{x}}$, the complex conjugation K, the sublattice exchange σ_x, and the local $U(1)$ gauge transformation $(\mathrm{e}^{\mathrm{i}\gamma})^{i_y}$. The invariance indicates that, under this composite operation, the Hamiltonian obeys $H = \Upsilon H \Upsilon^{-1}$, where the inverse operator is $\Upsilon^{-1} = (\mathrm{e}^{\mathrm{i}\gamma})^{i_y}\sigma_x K T_{\hat{x}}^{-1}$. It is easy to prove that the Υ operator satisfies

$$\Upsilon^2 = T_{2\hat{x}}, \quad (3)$$

where $T_{2\hat{x}}$ is a translation operator along the x direction by $2\hat{x}$.

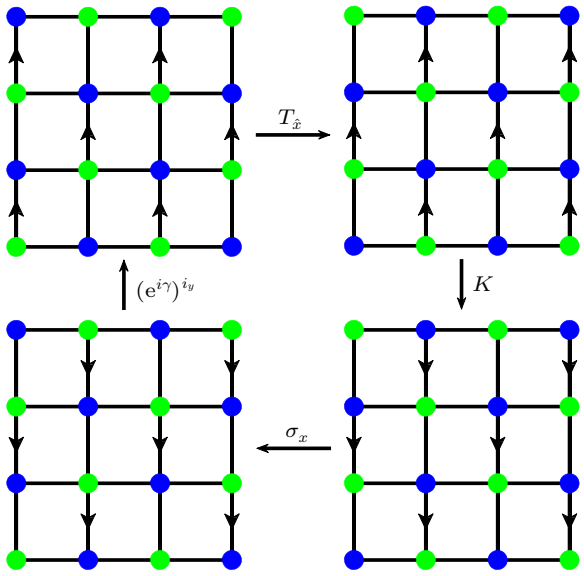


Fig. 2. The hidden symmetry of the lattice. The lattice keeps invariant after operated by the translation transformation $T_{\hat{x}}$, the complex conjugation K, the sublattice exchange σ_x, and the local $U(1)$ gauge transformation $(\mathrm{e}^{\mathrm{i}\gamma})^{i_y}$ in order. Here, the arrows represent a Peierls phase γ.

We take the Fourier transformation to the annihilation operators as

$$a_{\boldsymbol{k}} = \frac{1}{\sqrt{N}}\sum_i a_i \mathrm{e}^{-\mathrm{i}\boldsymbol{k}\cdot\boldsymbol{R}_i^A}, \quad (4)$$

$$b_{\boldsymbol{k}} = \frac{1}{\sqrt{N}}\sum_i b_i \mathrm{e}^{-\mathrm{i}\boldsymbol{k}\cdot\boldsymbol{R}_i^B}, \quad (5)$$

where N is the number of cells in the Bravais lattice. We define the two-component annihilation operator as $\eta_{\boldsymbol{k}} \equiv \frac{1}{\sqrt{2}}[a_{\boldsymbol{k}}, b_{\boldsymbol{k}}]^{\mathrm{T}}$, so that the Hamiltonian (1) can be rewritten as $H = \sum_{\boldsymbol{k}} \eta_{\boldsymbol{k}}^\dagger \mathcal{H}(\boldsymbol{k})\eta_{\boldsymbol{k}}$. Here, $\mathcal{H}(\boldsymbol{k})$ is the Bloch Hamiltonian

$$\mathcal{H}(\boldsymbol{k}) = -2t[\cos k_x + \cos(\gamma/2)\cos(k_y - \gamma/2)]\sigma_x - 2t\sin(\gamma/2)\cos(k_y - \gamma/2)\sigma_y, \quad (6)$$

where σ_x and σ_y are the Pauli matrices. Diagonalizing Eq. (6), we obtain the dispersion relation

$$E(\boldsymbol{k}) = \pm 2t\sqrt{\cos^2 k_x + \cos^2(k_y - \gamma/2) + 2\cos(\gamma/2)\cos k_x \cos(k_y - \gamma/2)}. \quad (7)$$

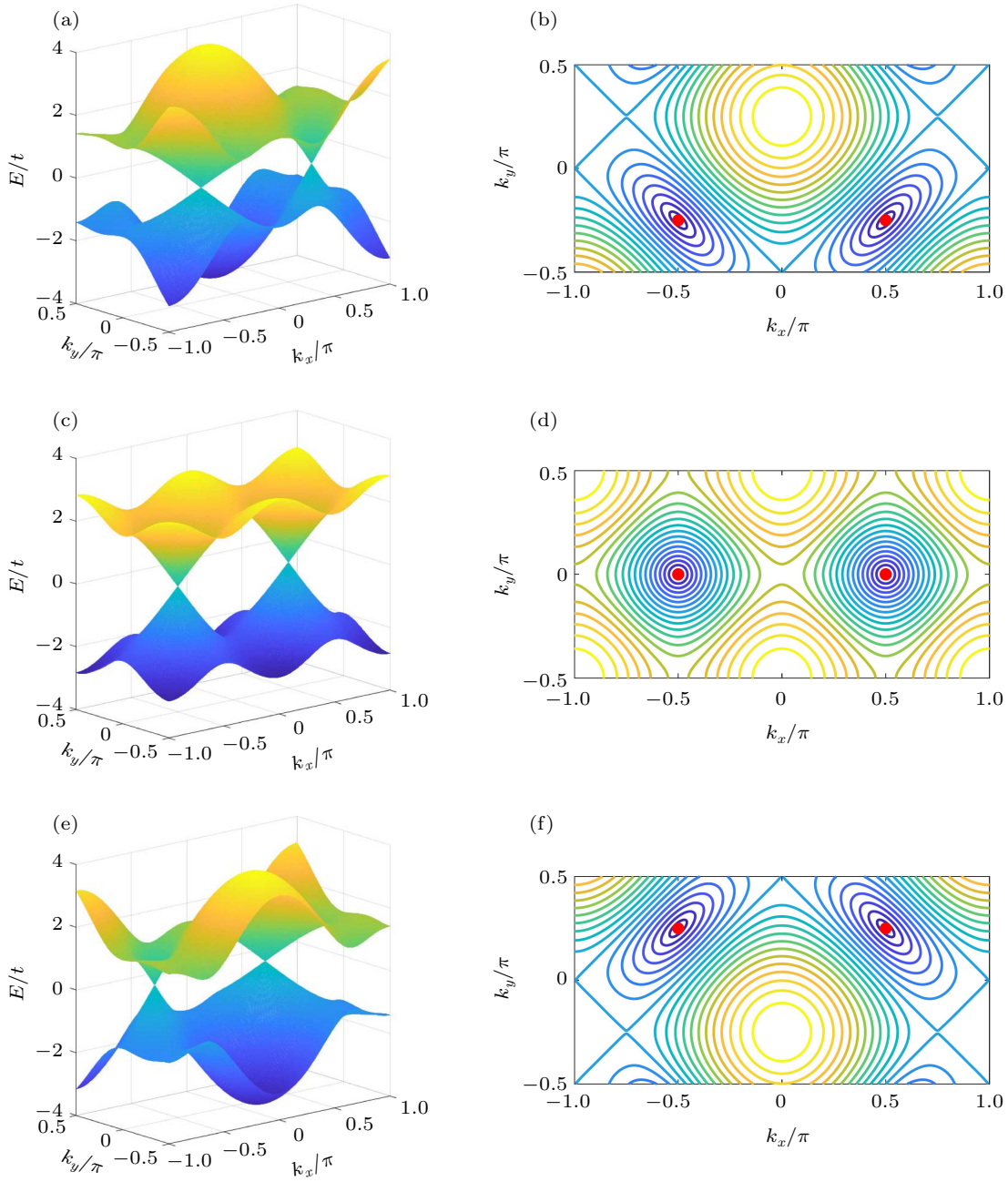


Fig. 3. The dispersion relations for different Peierls phases. Here, (a), (c), and (e) are the energy bands for the cases $\gamma = \pi/2, \pi$, and $3\pi/2$, respectively; (b), (d), and (f) are the energy contours of the conduction bands for the cases $\gamma = \pi/2, \pi$, and $3\pi/2$, respectively. In (b), (d), and (f), the red filled circles mark the positions of the Dirac points.

From the dispersion relation, we find that the conduction and valence bands touch at points $X_{1,2} = (\pm\pi/2, \gamma/2 - \pi/2)$ in the Brillouin zone as shown in Fig. 3 and the Bloch states at the band-touching points are degenerate. The Fermi surfaces are isolated points, so the system is a semimetal.

3. Topological semimetals and their properties

3.1. Topological semimetals

Here, we show that the semimetal in the system is a topological semimetal. The Bloch Hamiltonian (6) has the form $\mathcal{H}(\boldsymbol{k}) = \boldsymbol{h}(\boldsymbol{k}) \cdot \boldsymbol{\sigma}$ with $h_x(\boldsymbol{k}) = -2t[\cos k_x + \cos(\gamma/2)\cos(k_y - \gamma/2)]$ and $h_y(\boldsymbol{k}) = -2t\sin(\gamma/2)\cos(k_y - \gamma/2)$. We define a planar vector field $(\hat{h}_x(\boldsymbol{k}), \hat{h}_y(\boldsymbol{k}))$ in the Brillouin zone, where $\hat{h}_i(\boldsymbol{k}) = h_i(\boldsymbol{k})/|\boldsymbol{h}(\boldsymbol{k})|$ with $i = x, y$. The planar vector field $(\hat{h}_x(\boldsymbol{k}), \hat{h}_y(\boldsymbol{k}))$ is a unit vector field in a two-dimension space, so all the unit vectors form a one-dimensional manifold S^1. The Brillouin zone can be regarded as a torus manifold T. Thus, the planar unit vector field defines a mapping from T to S^1 as

$$\begin{aligned} \hat{\boldsymbol{h}}: \quad & T \to S^1, \\ & \boldsymbol{k} \mapsto (\hat{h}_x(\boldsymbol{k}), \hat{h}_y(\boldsymbol{k})). \end{aligned} \tag{8}$$

Based on the homotopy theory, this mapping can be classified by the winding numbers $\pi_1(S^1) = Z$, where Z is the set of all

integers.

The planar unit vector field $(\hat{h}_x(\boldsymbol{k}),\hat{h}_y(\boldsymbol{k}))$ has singularities at the band-touching points X_1 and X_2. The band-touching points can also be interpreted as topological defects, i.e., vortices, of the planar unit vector field. Concretely, around the band-touching points, the winding number can be calculated as follows:

$$w=\oint_{\mathcal{C}}\frac{\mathrm{d}\boldsymbol{k}}{2\pi}\cdot\left(\hat{h}_x\nabla\hat{h}_y-\hat{h}_y\nabla\hat{h}_x\right), \tag{9}$$

where ∇ is the differential operator in momentum space and $\mathcal{C}$ represents a closed path around one of the band-touching points. This winding number can be regarded as the topological charge of the defects. For the Bloch Hamiltonian (6), we calculate that the winding number is -1 and $+1$ for the vortices around the band-touching points X_1 and X_2, respectively. It turns out that X_1 and X_2 have opposite topological charges. It is obvious that the result about the topological charges obeys the fermion doubling theorem,[33] which states that topological point nodes in the energy spectrum of lattice Hamiltonians must come in pairs. When all paired opposite topological charges annihilate each other, a gap opens and the semimetal becomes an insulator. Due to the existence of the topological charges, so the semimetal is considered as a topological semimetal.

3.2. Dirac points

Near the band-touching points, the energy band has a cone-like shape and is linear. Around these band-touching points, the Bloch Hamiltonian (6) can be linearized as

$$h(\boldsymbol{p}) = 2t[\pm p_x-\cos(\gamma/2)p_y]\sigma_x-2t\sin(\gamma/2)p_y\sigma_y, \tag{10}$$

where $\boldsymbol{p}=\boldsymbol{k}-X_i$ with $i=1,2$; the two signs $\pm$ indicate the linearized Hamiltonian around the two distinct Dirac points X_1 and X_2, respectively. The quasiparticles behave like massless Dirac fermions. Thus, the band-touching points are Dirac points, around which are Dirac cones.

For Dirac cones in two dimensions, the chirality can be defined. For any Dirac cone in two dimensions, the Hamiltonian has the general form like $h(\boldsymbol{p})=\sum_{ij}v_{ij}p_i\sigma_j$, where v_{ij} are constant coefficients. One can define the chirality as $c=\mathrm{sgn}[\det(v_{ij})]=\pm1$ for the Dirac cone. From Eq. (10) and the definition of the chirality, we have $c=-1$ and $+1$ for the Dirac cones around the degenerate points X_1 and X_2, respectively. The results of chirality are consistent with the winding numbers for the Dirac points X_1 and X_2 calculated above. Thus, the chirality can be regarded as another definition of the topological charge.

3.3. Moving of Dirac points with the Peierls phase

For the system, the Peierls phase is a key parameter. The change of this parameter induces varying of the energy bands and moving of the Dirac points. In the Brillouin zone, the Dirac points locate at $X_{1,2}=(\pm\pi/2,\gamma/2-\pi/2)$, which are functions of the Peierls phase γ. When the Peierls phase γ varies, the Dirac points X_1 and X_2 move along two vertical lines in the Brillouin zone as shown in Fig. 1(b). For the case $\gamma=\pi$, the two Dirac points locate on the k_x axis and are symmetrical about the k_x and k_y axes. For the $0<\gamma<\pi$ case, the Dirac points locate on the lower half of the Brillouin zone, and for the $\pi<\gamma<2\pi$ case, the Dirac points locate on the upper half of the Brillouin zone. For the latter two cases, i.e., $\gamma\neq\pi$, the symmetry of the two Dirac points about the k_x axis is broken but the symmetry about the k_y axis is still preserved.

3.4. Anisotropy of Dirac cones

In the following, we show the relation between the shape of the Dirac cone and the Peierls phase. From the linearized Bloch Hamiltonian near the Dirac points, i.e., Eq. (10), one can find the quantum states with the non-zero eigenenergy E_0 that satisfies the equation

$$[\pm p_x-\cos(\gamma/2)p_y]^2+\sin^2(\gamma/2)p_y^2=\frac{E_0^2}{4t^2}. \tag{11}$$

We set

$$\alpha=\sqrt{|E_0/t|/[1\mp\cos(\gamma/2)]},$$
$$\beta=\sqrt{|E_0/t|/[1\pm\cos(\gamma/2)]},$$

then equation (11) is reformulated as

$$\frac{(p_x+p_y)^2}{\alpha^2}+\frac{(p_x-p_y)^2}{\beta^2}=1, \tag{12}$$

which is an elliptic equation and α (β) is the semi-major axis and β (α) is the semi-minor axis for the Dirac cone located around X_1 (X_2). That is to say, the closed curve formed by the intersecting of the constant-energy plance E_0 and the Dirac cone is an ellipse.

In order to depict the shape of the Dirac cones, we define an anisotropy factor with the eccentricity of the intersecting ellipse as

$$f=\sqrt{\frac{2|\cos(\gamma/2)|}{1+|\cos(\gamma/2)|}}, \tag{13}$$

which satisfies $0\leq f<1$, where $f=0$ indicates the isotropic case. The anisotropy factor is a function of the Peierls phase γ as shown in Fig. 4, which manifests that the shapes of the Dirac cones depend on the concrete value of the Peierls phase. When the Peierls phase γ is π, the anisotropy factor is vanishing, i.e., the intersecting curve is a circle and the Dirac cone is isotropic as shown in Fig. 3(d). when $\gamma\neq\pi$, we have $f>0$, which indicates that the intersecting curve is an ellipse and the Dirac cone is anisotropic as shown in Figs. 3(b) and 3(f). For the anisotropic cases, the massless Dirac fermions have different magnitudes of group velocities for any two non-coaxial directions.

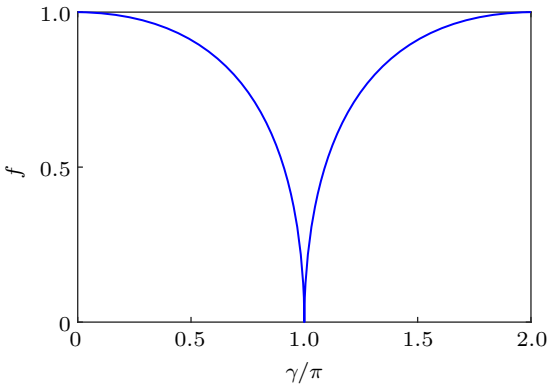


Fig. 4. The relation between the anisotropy factor of the Dirac cones and the Peierls phase.

4. Hidden symmetry protection

Here, we show that the Dirac points are protected by the hidden symmetry. Besides the second-quantized Hamiltonian H is invariant under the hidden symmetry operation, the single-particle Hamiltonian $H_{\rm s}$ also satisfies $H_{\rm s} = \Upsilon H_{\rm s} \Upsilon^{-1}$. In sublattice space, the Bloch function can be written as the two-component form

$$\Psi_{\boldsymbol{k}}(\boldsymbol{r}) = \begin{pmatrix} u_{\boldsymbol{k}}^{(1)}(\boldsymbol{r}) \\ u_{\boldsymbol{k}}^{(2)}(\boldsymbol{r}) \end{pmatrix} \mathrm{e}^{\mathrm{i}\boldsymbol{k}\cdot\boldsymbol{r}}. \tag{14}$$

When the symmetry operator Υ acts on the above Bloch function, based on its definition Eq. (2), we arrive at

$$\Upsilon\Psi_{\boldsymbol{k}}(\boldsymbol{r}) = \begin{pmatrix} u_{\boldsymbol{k}}^{(2)*}(\boldsymbol{r}-\hat{x})\,\mathrm{e}^{\mathrm{i}k_x} \\ u_{\boldsymbol{k}}^{(1)*}(\boldsymbol{r}-\hat{x})\,\mathrm{e}^{\mathrm{i}k_x} \end{pmatrix} \mathrm{e}^{-\mathrm{i}(\boldsymbol{k}-\gamma\boldsymbol{e}_{k_y})\cdot\boldsymbol{r}}, \tag{15}$$

where $\boldsymbol{e}_{k_y}$ is the unit vector along the k_y direction in reciprocal lattice space.

Because Υ is the symmetry operator of the system, $\Upsilon\Psi_{\boldsymbol{k}}(\boldsymbol{r})$ must be a Bloch wave function of the system and we denote it as $\Psi'_{\boldsymbol{k}'}(\boldsymbol{r}) \equiv \Upsilon\Psi_{\boldsymbol{k}}(\boldsymbol{r})$. Based on the definition Eq. (14), $\Psi'_{\boldsymbol{k}'}(\boldsymbol{r})$ has the form

$$\Psi'_{\boldsymbol{k}'}(\boldsymbol{r}) = \begin{pmatrix} u_{\boldsymbol{k}'}^{(1)}(\boldsymbol{r}) \\ u_{\boldsymbol{k}'}^{(2)}(\boldsymbol{r}) \end{pmatrix} \mathrm{e}^{\mathrm{i}\boldsymbol{k}'\cdot\boldsymbol{r}}. \tag{16}$$

Comparing Eq. (16) with Eq. (15), we obtain

$$\boldsymbol{k}' = \gamma\boldsymbol{e}_{k_y} - \boldsymbol{k}, \tag{17}$$

$$u_{\boldsymbol{k}'}^{(1)}(\boldsymbol{r}) = u_{\boldsymbol{k}}^{(2)*}(\boldsymbol{r}-\hat{x})\,\mathrm{e}^{\mathrm{i}k_x}, \tag{18}$$

$$u_{\boldsymbol{k}'}^{(2)}(\boldsymbol{r}) = u_{\boldsymbol{k}}^{(1)*}(\boldsymbol{r}-\hat{x})\,\mathrm{e}^{\mathrm{i}k_x}. \tag{19}$$

From Eq. (17), we know that, when the operator Υ acts on the wave vectors, it has the effect as $\Upsilon : \boldsymbol{k} \to \boldsymbol{k}' = \gamma\boldsymbol{e}_{k_y} - \boldsymbol{k}$.

If $\boldsymbol{k}' = \boldsymbol{k} + \boldsymbol{K}_m$, where $\boldsymbol{K}_m = m_1\boldsymbol{b}_1 + m_2\boldsymbol{b}_2$ is a reciprocal lattice vector, then we can say that $\boldsymbol{k}$ is a Υ-invariant point in momentum space. In the Brillouin zone, the Υ-invariant points are the points $Y_1 = (0, \gamma/2)$, $Y_2 = (0, \gamma/2 - \pi)$, and $X_{1,2} = (\pm\pi/2, \gamma/2 - \pi/2)$. Suppose that $\boldsymbol{G}$ represents a Υ-invariant point, then we have $\Upsilon\Psi_{\boldsymbol{G}}(\boldsymbol{r}) = \Psi'_{\boldsymbol{G}}(\boldsymbol{r})$. Because of the equation $\Upsilon H_{\rm s}\Upsilon^{-1} = H_{\rm s}$, $\Psi_{\boldsymbol{G}}(\boldsymbol{r})$ and $\Psi'_{\boldsymbol{G}}(\boldsymbol{r})$ are both the eigenstates of Hamiltonian $H_{\rm s}$ and have the same eigenenergy $E_{\boldsymbol{G}}$. After the symmetry operator acts on the Bloch function two times, we have

$$\Upsilon^2\Psi_{\boldsymbol{G}}(\boldsymbol{r}) = T_{2\hat{x}}\Psi_{\boldsymbol{G}}(\boldsymbol{r}) = \mathrm{e}^{-2\mathrm{i}G_x}\Psi_{\boldsymbol{G}}(\boldsymbol{r}), \tag{20}$$

where G_x is the x component of $\boldsymbol{G}$ and equation (3) is used for the derivation of the first equality. From the above equation, we obtain $\Upsilon^2 = \mathrm{e}^{-2\mathrm{i}G_x}$, which is a function of the wave vector. Substituting the wave vectors of the Υ-invariant points $Y_{1,2}$ and $X_{1,2}$, we obtain $\Upsilon^2 = 1$ at $Y_{1,2}$ and $\Upsilon^2 = -1$ at $X_{1,2}$. If a system is invariant under the action of an antiunitary operator and the square of the operator is not equal to 1, there must be degeneracy protected by this antiunitary operator.[34] Thus, the quantum states must be degenerate at the points $X_{1,2}$ in the Brillouin zone, which means that the energy bands must touch at the points $X_{1,2}$. This result is consistent with the Dirac points obtained from the dispersion relation. Therefore, the hidden symmetry is responsible to the energy degeneracy at the Dirac points. Because the hidden symmetry Υ is dependent on the Peierls phase, the Υ-invariant points are functions of the Peierls phase. Thus, the variation of the Peierls phase leads to the change of the hidden symmetry. Further, the change of the hidden symmetry results in moving of the Dirac points in the Brillouin zone.

5. Feasibility of experimental realization

Due to the great development of ultracold atom and optical lattice techniques in recent years, it is possible to realize the model and to detect the results experimentally. There are two key points in the physical realization of the model. The first key point is to generate the hopping-accompanying phase, i.e., the Peierls phase. The existing techniques provide several methods to generate the Peierls phase. One of the methods is the laser-assisting tunneling technique,[17,18] which is extensively used to produce Peierls phases or gauge fields in optical lattice. Another method to generate Peierls phase is the shaking optical lattice technique.[19,20] The second key point is to detect the band structure. An available detecting technique is Bragg spectroscopy,[35,36] which has been employed in several schemes to detect the band structure of edge states and bulk states.[25,37–39] Thus, it is feasible to realize the model in optical lattices with the existing ultracold atom techniques.

6. Conclusion

In summary, we have presented a square lattice with a Peierls phase for some neighbor hoppings, which can be realized with ultracold atoms in optical lattices. Because of the existence of the Peierls phase, the translation symmetry is broken

and the system has a special band structure. Two Dirac points exist in the Brillouin zone and the Dirac points move with the change of the Peierls phase. When the Peierls phase is π, the Dirac cones are isotropic, and when the Peierls phase has other value in the ranges $(0,\pi)$ and $(\pi,2\pi)$, the Dirac cones are anisotropic, the anisotropy factor was defined to depict the anisotropy of the Dirac cones. It was shown that the lattice has a special hidden symmetry, which is a composite antiunitary symmetry. The hidden symmetry protects the Dirac points and the moving of Dirac points in the Brillouin zone is perfectly explained by the hidden symmetry protection. Finally, we discussed the feasibility of the realization of the lattice with ultracold atom and optical lattice techniques.

References

[1] Hasan M Z and Kane C L 2010 *Rev. Mod. Phys.* **82** 3045
[2] Qi X L and Zhang S C 2011 *Rev. Mod. Phys.* **83** 1057
[3] Wan X, Turner A M, Vishwanath A and Savrasov S Y 2011 *Phys. Rev. B* **83** 205101
[4] Xu G, Weng H, Wang Z, Dai X and Fang Z 2011 *Phys. Rev. Lett.* **107** 186806
[5] Burkov A A, Hook M D and Balents L 2011 *Phys. Rev. B* **84** 235126
[6] Burkov A A and Balents L 2011 *Phys. Rev. Lett.* **107** 127205
[7] Fang C, Gilbert M J, Dai X and Bernevig B A 2012 *Phys. Rev. Lett.* **108** 266802
[8] Zyuzin A A, Wu S and Burkov A A 2012 *Phys. Rev.* **85** 165110
[9] Jaksch D and Zoller P 2005 *Ann. Phys.* **315** 52
[10] Lewenstein M, Sanpera A, Ahufinger V, Damski B, Sen A and Sen U 2007 *Adv. Phys.* **56** 243
[11] Bloch I, Dalibard J and Zwerger W 2008 *Rev. Mod. Phys.* **80** 885
[12] Cooper N R, Dalibard J and Spielman I B 2019 *Rev. Mod. Phys.* **91** 015005
[13] Greiner M, Mandel O, Esslinger T, Hänsch T W and Bloch I 2002 *Nature* **415** 39
[14] Jaksch D, Bruder C, Cirac J I, Gardiner C W and Zoller P 1998 *Phys. Rev. Lett.* **81** 3108
[15] Hou J M and Ge M L 2003 *Phys. Rev. A* **67** 063607
[16] Lin Y J, Compton R L, Jiménez-García K, Porto J V and Spielman I B 2009 *Nature* **462** 628
[17] Aidelsburger M, Atala M, Nascimbène S, Trotzky S, Chen Y A and Bloch I 2011 *Phys. Rev. Lett.* **107** 255301
[18] Miyake H, Siviloglou G A, Kennedy C J, Burton W C and Ketterle W 2013 *Phys. Rev. Lett.* **111** 185302
[19] Struck J, Ölschläger C, Weinberg M, Hauke P, Simonet J, Eckardt A, Lewenstein M, Sengstock K and Windpassinger P 2012 *Phys. Rev. Lett.* **108** 225304
[20] J Struck, Weinberg M, Ölschläger C, Windpassinger P, Simonet J, Sengstock K, Höppner R, Hauke P, Eckardt A, Lewenstein M and Mathey L 2013 *Nat. Phys.* **9** 738
[21] Trotzky S, Cheinet P, Fölling S, Feld M, Schnorrberger U, Rey A M, Polkovnikov A, Demler E A, Lukin M D and Bloch I 2008 *Science* **319** 295
[22] Eckardt A, Hauke P, Soltan-Panahi P, Becker C, Sengstock K and Lewenstein M 2010 *Europhys. Lett.* **89** 10010
[23] Simon J, Bakr W S, Ma R, Tai M E, Preiss P M and Greiner M 2011 *Nature* **472** 307
[24] Greif D, Uehlinger T, Jotzu G, Tarruell L and Esslinger T 2013 *Science* **340** 1307
[25] Hou J M, Yang W X and Liu X J 2009 *Phys. Rev. A* **79** 043621
[26] Lim L K, Smith C M and Hemmerich A 2008 *Phys. Rev. Lett.* **100** 130402
[27] Goldman N, Kubasiak A, Bermudez A, Gaspard P, Lewenstein M and Martin-Delgado M A 2009 *Phys. Rev. Lett.* **103** 035301
[28] Bercioux D, Urban D F, Grabert H and Häusler W 2009 *Phys. Rev. A* **80** 063603
[29] Sun K, Liu W V, Hemmerich A and Das Sarma S 2012 *Nat. Phys.* **8** 67
[30] Hou J M 2013 *Phys. Rev. Lett.* **111** 130403
[31] Goldman N, Anisimovas E, Gerbier F, Öhberg P, Spielman I B and Juzeliūnas G 2013 *New J. Phys.* **15** 013025
[32] Mai X Y, Zhang D W, Li Z and Zhu S L 2017 *Phys. Rev. A* **95** 063616
[33] Nielsen H B and Ninomiya M 1981 *Nuclear Physics B* **185** 20
[34] Hou J M and Chen W 2018 *Front. Phys.* **13** 130301
[35] Stenger J, Inouye S, Chikkatur A P, Stamper-Kurn D M, Pritchard D E and Ketterle W 1999 *Phys. Rev. Lett.* **82** 4569
[36] Steinhauer J, Ozeri R, Katz N and Davidson N 2002 *Phys. Rev. Lett.* **88** 120407
[37] Stanescu T D, Galitski V and Das Sarma S 2010 *Phys. Rev. A* **82** 013608
[38] Liu X J, Liu X, Wu C and Sinova J 2010 *Phys. Rev. A* **81** 033622
[39] Goldman N, Beugnon J and Gerbier F 2012 *Phys. Rev. Lett.* **108** 255303